Optimized Electric Propulsion System Modeling and Simulation with Low Voltage DC Hybrid Power Systems

N.Visali[1], S.Niranjan[2]

Professor and HOD, M.Tech, Ph.D. Dept. of E.E.E, JNTU Engineering College, Pulivendula, Kadapa, A.P, India[1]

PG Student (EPS), Dept. of E.E.E, JNTU Engineering College, Pulivendula, Kadapa, A.P, India[2]

ABSTRACT: Electrification of ship propulsion system with hybrid power systems created interest in modeling of all marine vessels. Reduction in the emission of green house gases, fuel consumption and efficient energy management with improved system dynamic performance is possible with hybrid power systems. With penetration of power electronic converters into power systems, ship board direct current distribution systems offer further more advantages such as space, weight saving and flexible arrangement of equipment. On board marine vessel consists of synchronous generator, energy storage system, fuel cell, photo voltaic array and induction motor drive. Power electronic converters are modeled through detailed model. Mechanical components are modeled with mathematical analysis approach. Power sharing among the proposed hybrid power system is observed in MATLAB/Simulink software**.**

KEYWORDS: Simulation, DC distribution systems, detailed modeling, PVA module, and vector (or) field oriented control.

NOMENCLATURE

A	Curve fitting factor	v	Voltage.
d	Instantaneous duty cycle.	w	Taylor's wake fraction.
D	Design value of duty cycle.	ρ	Water density.
$d_{a,b,c}$	Switching functions of the inverter.	ψ	Flux linkage.
D_p	Propeller diameter.	e	Electron charge (1.602×10^{-19} C).
ESS	Energy storage system.	K	Boltzmann constant (1.38×10^{-23} J/^{0}K).
FC	Fuel cell.	I_c	Cell output current, A.
PVA	photo voltaic array	I_{ph}	Photo current.
K_q	Propeller torque coefficient.	I_0	Reverse saturation current of diode (0.0002 A).
K_t	Propeller thrust coefficient.	T_c	Reference cell operating temperature (20 °C).
m	Modulation index.	V_c	Cell output voltage.
n	Transformer turns ratio.	SOC	State of charge.
Q_p	Propeller torque.		
T_p	Propeller thrust.		

I.   INTRODUCTION

Electrical installations are present in every marine vessel ranging from powering of communication and monitoring systems, running of different motors to high power electrical installation for electric propulsion [1]-[2]. With the possibility to control electrical motors with variable speed drives in a large power range with compact, reliable and cost competitive solutions, the use of electrical propulsion has emerged in new application areas. Electrification of propulsion system brought us advantages like improved life cycle cost by reduced fuel consumption and maintenance, less propulsion noise and vibrations, Less space consuming etc[3]-[5].

Now a day's all electrical ships are enabled by hybrid power systems [6]. Hybrid power systems use low calorie renewable energy resources to generate electrical energy [7]-[9]. In this paper hybrid power system incorporates a set of primary and auxiliary energy sources in order to provide the propulsion power and at the same time, to energize the ship board electric loads. A gas or diesel energy source comes under primary sources which are capable to drive both propulsion and also ship loads. Fuel cell, photo voltaic, and energy storage systems comes under auxiliary sources which participate only in improving ship dynamic performance and also ship load system.

Models are derived for different electrical and mechanical elements including the synchronous generator–rectifier system, inverter, dc/dc converters, diesel engine, propeller, and ship hydrodynamics. Power electronic converters are modeled in detailed modeling to give an effective solution and to improve speed of simulation. A simulation platform is developed in MATLAB/Simulink for system-level studies of hybrid electric ships. As a case study, marine vessel is simulated in different modes of operation. The simulation results of a power sharing control among two diesel generators, a fuel cell unit, photo voltaic array and an energy storage system show practical utility of such a simulation tool in system studies associated with design, evaluation, power management.

II.   SYSTEM CHARACTERISTICS AND OVERVIEW
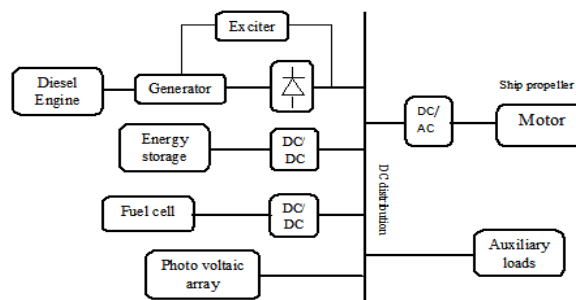
Fig. 1 Single line diagram of shipboard DC hybrid power system

The single line diagram of an overall system is shown in the above Fig. 1. Modeling of system-level analysis of ship dc distribution power systems requires specific features imposed by the system characteristics. First of all, there are mechanical and electrical components in such a system with extremely different dynamics. This difference ranges from a very small time constant of a power electronic switch, which is on the order of nanoseconds to a large time constant of ship hydrodynamics, which is tens of seconds. Detailed switching models of power electronic converters are considered hear. Second, for system level studies, in which large variations occur in system states, small signal or linearized averaging is invalid, and large signal models must be developed instead. Third, the interactions among connected elements should be included in order for the system model to be realistic. In other words, each element should receive the reaction of the connected elements, as soon as it affects them.

III.   MODELING OF POWER ELECTRONIC CONVERTERS

It is the power electronics, area that brought a great change in technology of electric power industry. Compared to rotating commutation static conversion is more efficient and reliable. The DC-DC converters are very prominent for energy management in shipboard hybrid power systems [10]. These converters are used to shift voltage from one level to another among the dc distribution system. Here we use two types of DC-DC converters, a boost converter to step up the voltage generated from fuel cell module and a boost type bidirectional converter for battery cell module.

A.   DC-DC Boost Converter
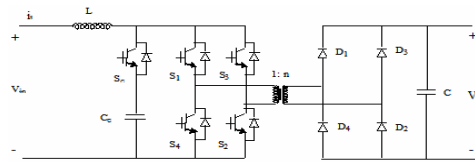
Fig. 2 Full-Bridge boost converter circuit

The step up dc to dc converter is basically called as boost converter [10]. Topological circuit diagram of full bridge boost converter is shown in above fig.2. Here we can observe that when controllable switch (S_c) is in 'on' state, current flows through inductor and it charges. When switch is in 'off' state the energy stored inductor and supply voltage together gets voltage boost. The amount of boosting voltage depends on duty cycle of controllable switch.

B. DC-DC Bi-Directional Converter
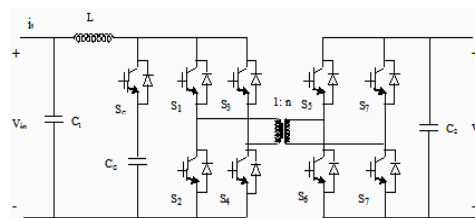
Fig. 3 Full-Bridge bidirectional converter circuit

Most of the existing bidirectional dc-dc converters fall into the generic circuit structure illustrated in the above fig. 3 which is characterized by a current fed or voltage fed on one side. Based on the placement of the auxiliary energy storage, the bidirectional dc-dc converter can be categorized into buck and boost type [12]. The buck type is to have energy storage placed on the high voltage side, and the boost type is to have it placed on the low voltage side [11]. The high frequency transformer based system is an attractive one to obtain isolation between the source and load sides, since transformer can isolate the voltage sources and provide the impedance matching between them.

C. Synchronous Machine-Rectifier System

Nearly all of the electrical power used throughout the world is generated by the synchronous machines driven either by steam or hydraulic turbine or any combustion engines. The synchronous machine is the principle means of converting mechanical energy to electrical energy [13]. Here we prefer d-q model to eliminate the dependency of inductance on rotor position. Since rotor field, d and q-axis are already aligned in rotor coordinates it is only stator voltages, currents and flux linkages that have to be transformed to the rotor coordinates [14]. This transformation is done through park's transformation, valid for voltages, currents, and flux linkages.

$$[P(\theta_{er})] = \frac{2}{3}\begin{bmatrix} \cos(-\theta_{er}) & \cos(-\theta_{er} + \frac{2\pi}{3}) & \cos(-\theta_{er} - \frac{2\pi}{3}) \\ \sin(-\theta_{er}) & \sin(-\theta_{er} + \frac{2\pi}{3}) & \sin(-\theta_{er} - \frac{2\pi}{3}) \\ \frac{1}{2} & \frac{1}{2} & \frac{1}{2} \end{bmatrix} \tag{1}$$

$$\begin{bmatrix} v_d \\ v_q \\ v_0 \end{bmatrix} = [P(\theta_{er})].\begin{bmatrix} v_A \\ v_B \\ v_C \end{bmatrix} \quad ; \quad \begin{bmatrix} I_d \\ I_q \\ I_0 \end{bmatrix} = [P(\theta_{er})].\begin{bmatrix} I_A \\ I_B \\ I_C \end{bmatrix} \quad ; \quad \begin{bmatrix} \psi_d \\ \psi_q \\ \psi_0 \end{bmatrix} = [P(\theta_{er})].\begin{bmatrix} \psi_A \\ \psi_B \\ \psi_C \end{bmatrix} \tag{2}$$
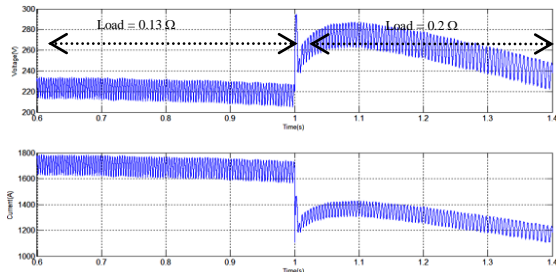
Fig. 4 SM-rectifier response to a step change at higher loads
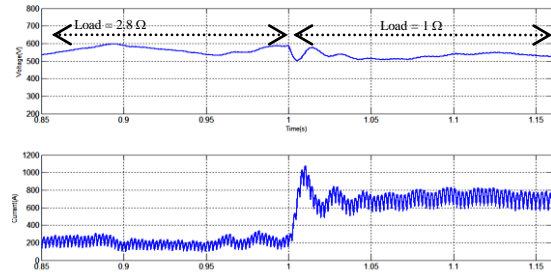
Fig.5 SM-rectifier response to a step change at lower loads

As a case study synchronous machine rectifier system is modeled in detailed model. The response to a step change in the higher loads (0.13Ω to 0.2Ω) is also shown in the above fig. 4. Similarly for a step change in the lower loads (2.8Ω to 1Ω) is observed here in the above fig. 5. Modeling of the synchronous machine in the detailed model gives us better precision than any other average value models with constant and also variable parameters.

D. Modeling of induction motor drive

Induction motor drives have been the work horses for variable speed applications ranging from fractional horse power to multi-megawatt. Modeling of induction motor drive is done in vector control method, though scalar control method is simple to implement, due to its inherent coupling effect gives sluggish response and the system is prone to instability. A vector controlled induction motor drive operates like a separately exited dc motor drive [14].

IV.   MODELING OF PHOTO VOLTAIC ARRAY

Photo voltaic solar cells (PVSC) are emerging as a renewable green energy power source. Use of solar energy gives reduces fuel consumption and emission of green house gases. Combined series/parallel combinations of photo voltaic solar cells, which are usually represented by a simplified equivalent circuit model shown in below fig. 6 or by equation 3.
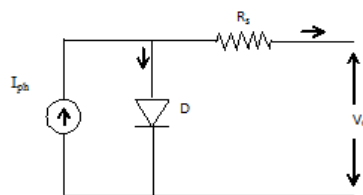
Fig.6 Simplified circuit of photo voltaic cell

$$V_c = \frac{AkT_c}{e} ln\left(\frac{I_{ph}+I_0-I_c}{I_0}\right) - R_s I_c \qquad (3)$$

The above equation gives single solar cell voltage which is then multiplied by number of cells connected in series to get full array voltage [15]. The solar cell operating temperature varies as a function of solar irradiation and level and ambient temperature (Ta). These effects are represented in the model by temperature coefficients C_{TV} and C_{TI} for cell output voltage and current.

$$C_{TV} = 1 + \beta_T(T_a - T_X) \quad \text{- (4)} \qquad\qquad C_{T1} = 1 + \frac{\gamma_T}{S_c}(T_X - T_a) \qquad \text{- (5)}$$

Where $\beta_T = 0.004$ and $\gamma_T = 0.06$ for the cell used $T_a=20^0c$ is the ambient temperature during cell testing. This is used to obtain the modified model of cell for another ambient temperature T_x. If solar irradiation (S_c) increases from S_{x1}

to S_{x2} the cell operating temperatures and currents also increases to new values. Thus this change due to solar irradiation can be implemented using correction factors.

$$C_{SV} = 1 + \beta_T \alpha_S (S_x - S_C) \text{ - (6)} \qquad C_{T1} = 1 + \frac{1}{S_c}(S_x - S_C) \text{ - (7)} \qquad \Delta T_C = \alpha_S (S_x - S_C) \text{ - (8)}$$

Where S_c is the original solar irradiation level and S_x is the new level. C_{SI}, C_{SI} are correction factors for cell output voltages and currents and ΔT_C is the change in the temperature with α_S slope change in the operating temperature. By using all correction factors new output voltage V_{CX} and photo current I_{phx} are obtained as follows:

$$V_{CX} = C_{TV} C_{SV} V_C \quad , \quad I_{phx} = C_{TI} C_{SI} I_{ph} \tag{9}$$
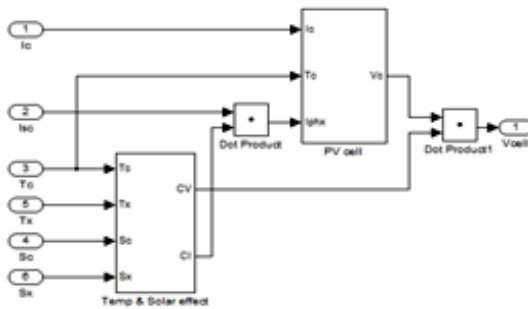
Fig.7 Stage 1 modeling photo voltaic
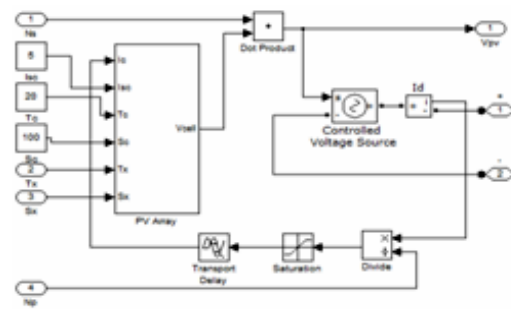
Fig.8 Modeling stage 2 of photo voltaic array

Here above fig. 7 is the sub model of the photo voltaic array block in above fig. 8.

V. MODELING OF MECHANICAL SYSTEMS

1. *Propeller Modeling*

Propeller can be modeled by implementing relations between torque, thrust and speed. For fixed propeller these relationships can be expressed as given below eq. 10 and eq.11 [16].

$$T_p = \rho D_p^4 K_T n_m \qquad \text{- (10)} \qquad Q_p = \rho D_p^5 K_Q n_m \qquad \text{- (11)}$$

Where T_p is propeller thrust [N]. n_m is the propeller shaft speed [rpm], and Q_p is the propeller torque [N-m]. Parameters ρ. D_p, K_T and K_Q are water density, propeller diameter, thrust coefficient, respectively. K_T and K_Q are functions of propeller structure and advance ratio J and advance velocity V_A is always less than the ship velocity due to Taylor's wake fraction (w). Their relations are expressed by

$$J = \frac{V_A}{n_m D_P} \qquad \text{- (12)} \qquad V_A = V_S(1 - w) \text{ - (13)}$$

2. *Ship Hydro Dynamics*

The vessel hydrodynamic model could be complicated when dynamic positioning is purposed [17]. For power system analysis in integrated power and propulsion systems, a one dimensional forward-motion model suffices.

Therefore, the ship can be treated as an inertial mass with a resistive drag, on which the propeller thrust T_p applies. The resistive drag is proportional to the square of ship speed V_s.

3. Diesel Engine

Diesel engine dynamics can be modeled in different levels of complexity, depending on the application. In this paper, it is approximated by a time delay τ and a time constant τ_C [16] as represented in (14).

$$T_m(S) = e^{-\tau s} \frac{K_y}{1+\tau_c s} Y(s) \qquad (14)$$

Where T_m is the generated torque, K_y is the torque constant, and *Y* is the fuel index (governor setting). The time delay is half the period between consecutive cylinder firings, which can be calculated by eq. 15 [37].

$$\tau \approx \frac{1}{2n_m N} \qquad - (15) \qquad\qquad \tau_c \approx \frac{0.9}{2n_m \pi} \qquad - (16)$$

Where n_m is the engine rotational speed in [rps] and N is the number of cylinders. The time constant is calculated by eq.16.In order to model the interaction between the diesel engine and the synchronous generator, a speed control loop is established between speed governor and synchronous generator.

VI. SYSTEM SIMULATION AND RESULTS

The below fig. 9 represents overview of the system implemented in MATLAB/Simulink. Interfaces among elements are bidirectional to represent interactions among connected elements. This facilitates the interface among different types of electrical, mechanical, and electromechanical elements. Parameters for different parts of the system are given in the Appendix. To represent the simulation results, a sailing profile including high speed (140 rad/sec), moderate speed (70 rad/se), and low speed (30 rad/sec) is studied in this section with and without solar module.
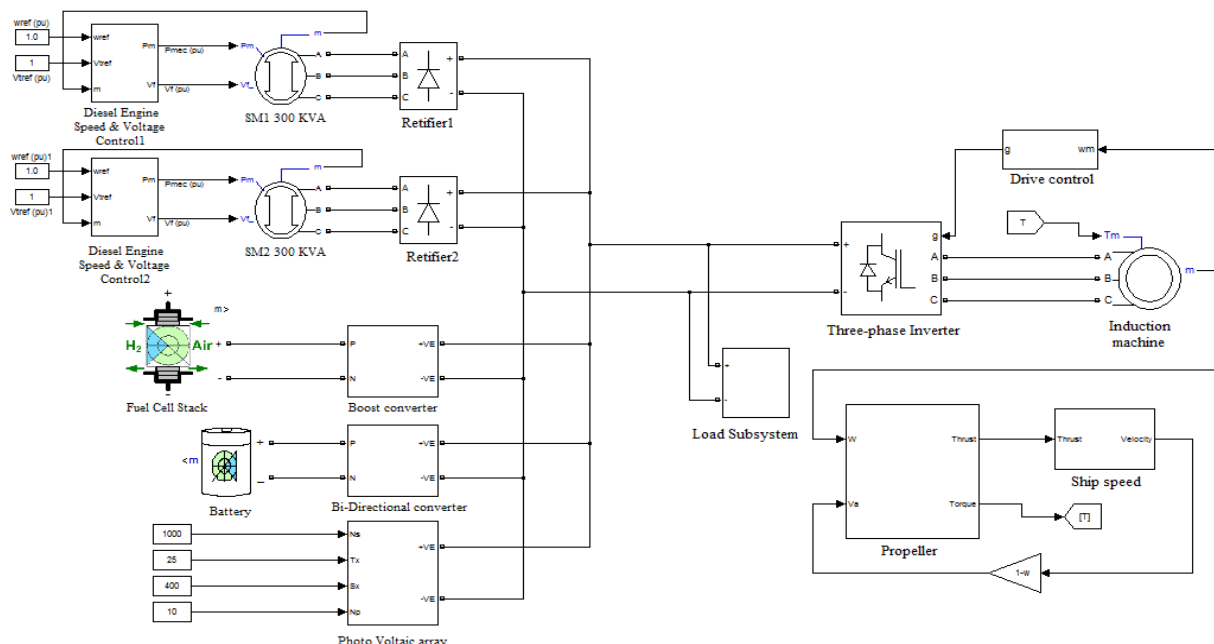
Fig.9 Overview of ship hybrid power system implemented in MATLAB/Simulink

A.   Without solar module under operation
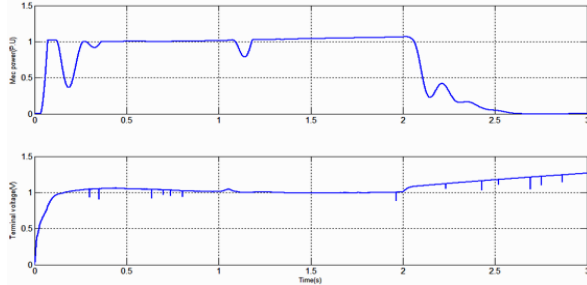
Fig.10 (a) (b) Per unit mechanical power and terminal voltage of generator-1
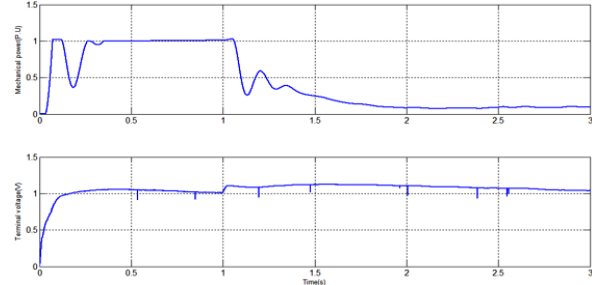
Fig.11 (a) (b) Per unit mechanical power and terminal voltage of generator-2

Fig. 10 (a), (b) shows per unit mechanical power and terminal voltage of generator set-1. Fig. 11 (a), (b) shows per unit mechanical power and terminal voltage of and generator set-2.

Fig. 12(a) shows the variation in the stator current of motor used for propulsion. Fig. 12(b) represents ship actual speeds and reference speeds of propulsion motor. Fig. 12(c) represents propeller reference torque and electromagnetic torque of induction motor over the simulation time.
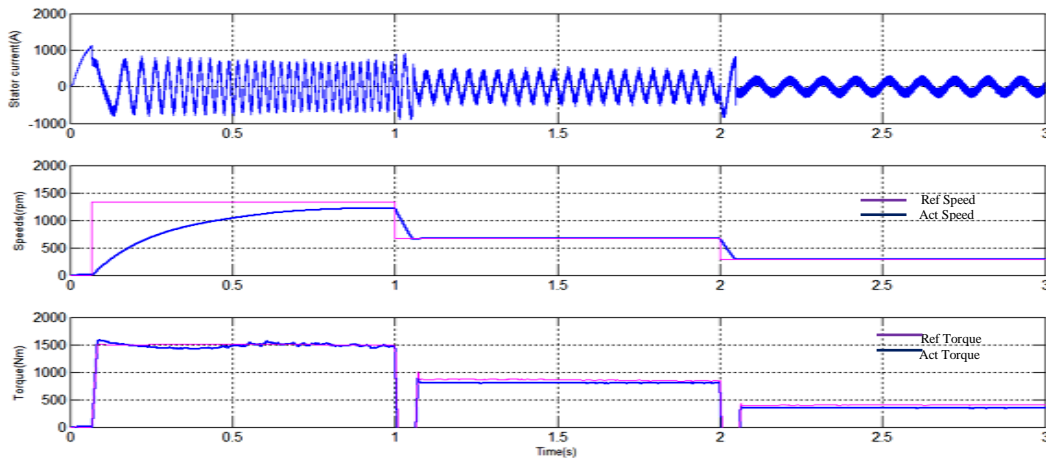
Fig.12 (a), (b), (c) Stator current, speeds, and torques of induction machine

.

In the first cycle, the ship is accelerating from zero to full speed, which examines the power system response to high stress and also due to high inertia during start current drawn during this cycle of operation is high. The propeller accelerates much faster than the ship, as dynamics of the propulsion system is much faster than ship motion so during first cycle there is a deviation of the actual speed from reference speed, but in later cycles of operation both speeds are same with small deviations. In reference electromagnetic torque and actual electromagnetic torque of the propulsion induction motor there is minor deviation between these two torques which is due to load variation during first cycle is high i.e. from zero to maximum torque value, so variation between torques is more in first cycle of operation. In remaining two stages of operation better match is obtained between reference torque and actual torque.
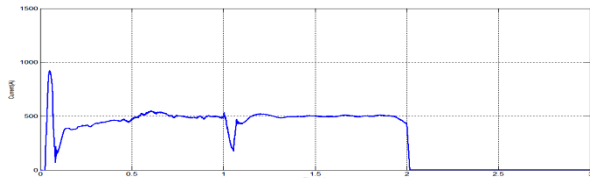
Fig.13 Current of generator-1
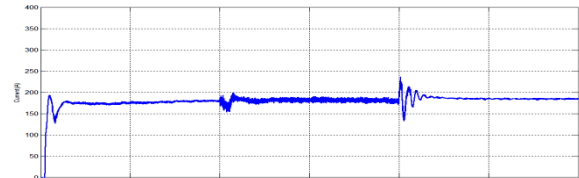
Fig.15 Current of fuel cell
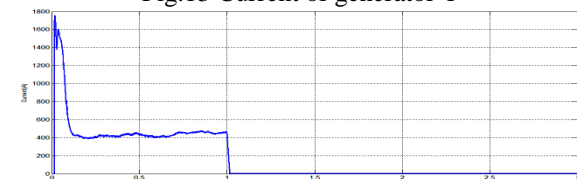
Fig.14 Current of generator-2
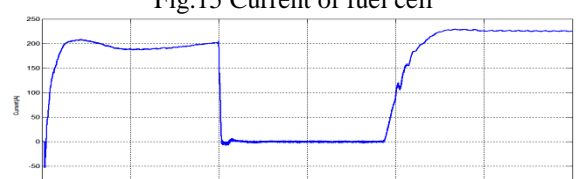
Fig.16 Current of battery

Fig. 13 to fig.16 shows dc currents of different units that are connected to the dc grid. During high speeds 140 rad/sec, the propulsion system demands highest amount of power. Therefore, both of the diesel generators, the fuel cell, and the energy storage supply power to the grid during the first cycle of simulation. The propulsion power highly reduces with the reduction of propeller rotational speed and ship speed.
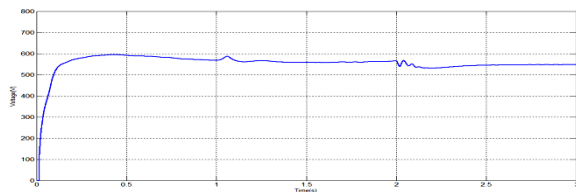
Fig. 17 DC bus voltage
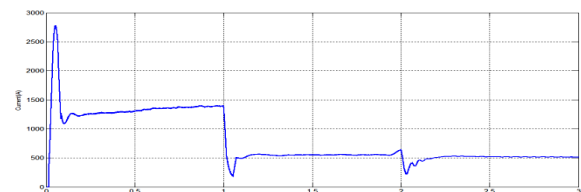
Fig. 18 Total load current

Reduction of the ship speed by half leads to reduction in the propeller speed. At this speed range 70 rad/sec, one of the generators (G2) shuts down and the power is mainly supplied by the remaining generator (G1) and the fuel cell. At slow speed operation (30 rad/sec), the generator G1 also shuts down, and the power is mainly supplied by the fuel cell, and battery.
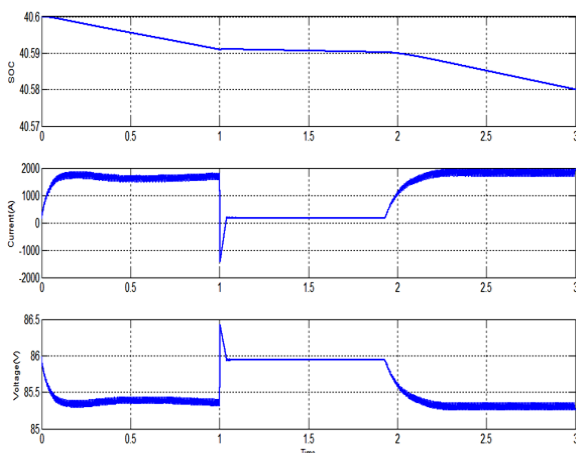
Fig. 19 Battery SOC, Current and Voltage
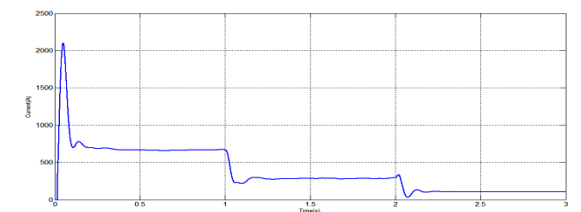
Fig.20 Auxiliary load current
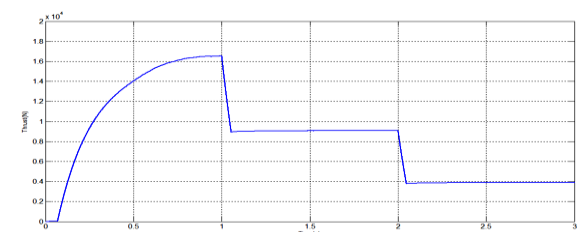
Fig.21 Thrust

Fig. 17 shows the dc bus voltage which is maintained constant with small droop. Fig. 18 shows total load current drawn by overall system. The battery state of charge (SOC) is maintained within certain limits. This is done by starting an idle diesel generator when SOC reaches the lower boundary, and by shutting down an active diesel generator when SOC exceeding the upper limit. Fig. 18 shows SOC, voltage, and current of the battery. Fig.20 shows load current of ship auxiliary and hotel load rated at 175hp, which is modeled by a constant dc motor load.

B.   With solar module under operation

This addition of solar module provides ultra-low emission mode of operation, which is important when ship is approaching/leaving harbors at low speeds. Improvement in voltage profile is observed with addition of additional solar module. Some of important waveforms are shown below.
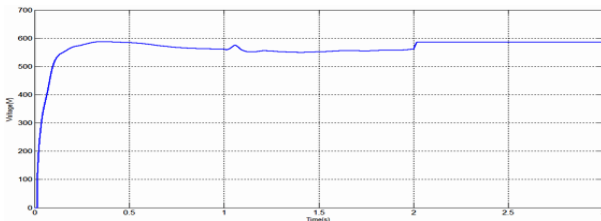
Fig. 22 DC bus voltage with solar module
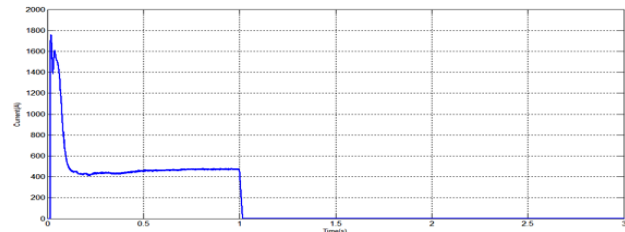
Fig. 24 Current of generator-2
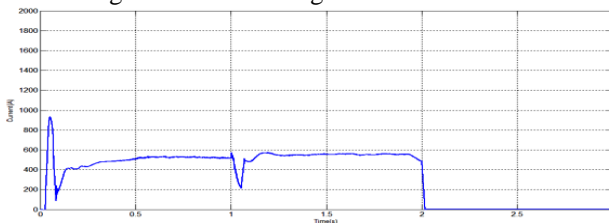
Fig.23 Current of generator-1
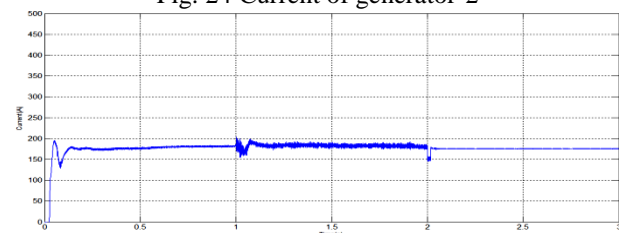
Fig.25 Current of fuel cell

Fig. 22 shows the dc bus voltage which is maintained constant with small droop we can observe the improvement in voltage profile with additional hybrid power system. Fig. 23 to fig.27 shows dc currents of different units that are connected to the dc grid. Since there is no change in load pattern the electromagnetic torque, thrust, auxiliary load current and total load current drawn will remains same as shown in the above case without solar module under operation.
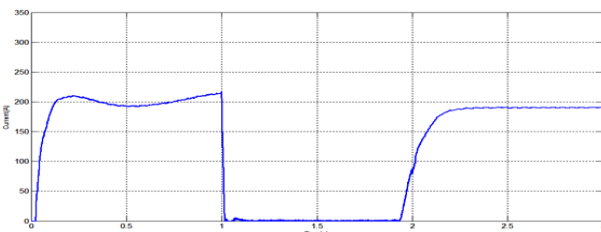
Fig.26 Current of battery

Fig. 27 Photo voltaic array current

The control methods for power sharing and voltage regulation of all-electric ships with dc distribution systems can be tested and optimized by this simulation program. The derived models and the simulation platform can be reconfigured to assist in design, implementation, and control of experimental setups of dc power systems for all-electric ships.

VII.   CONCLUSION

A simulation platform is developed using the derived models of different components presented in the paper. Detailed modeling method is used to model all power electronic converters without neglecting system dynamic behavior. We have observed the exact system behavior under transient conditions. The simulation results for a sailing profile of an all-electric ship and how power sharing is done between different mechanical and electrical components with different dynamics. A significant reduction in emission of green house gases and use of non-renewable energy (diesel) is done by adding a green energy source so that better energy management is done and improvement in voltage profile is obtained. With this green power sources ultra low emission of effluent gases like near shore is obtained.

APPENDIX

1) The synchronous generator model is based on Park's equivalent circuit [14] with the following parameters: 300 KVA, 320/460 V, 2 pole pairs, $J = 3.35$ kg.m^2, $r_s = 16.6$ mΩ, $r_{fd} = 5.245$ mΩ, $L_{lfd} = 0.68$ mH, $L_{ls} = 16.8$ mH, $L_{md} = 5.85$ mH, $L_{mq} = 5.05$ mH, $r'_{kd1} = 0.1526$ Ω, $L'_{lkd1} = 3.404$ mH, $L'_{lkq1} = 3.404$ mH, $r'_{kq1} = 40.57$ mΩ.

2) Fuel cell parameters: 130 cells, $V_{nom} = 90$ V, $I_{nom} = 1333$ A, $I_{max} = 2250$ A, $T = 700^0$C, $P = 119.9$ kW.

3) Li-ion battery parameters: $V_{full} = 93.1$ V, $V_{nom} = 80$ V, 5 kAh.

4) The induction motor is modeled in synchronously rotating d-q reference frame [46] using the following parameters: 200 hp, 320/460 V, 4 poles, $J = 4.1$ kg·m^2, $r_s = 7.6$ mΩ, $R'_r = 4.6$ mΩ, $L_{ls} = 0.15$ mH, $L'_{lr} = 0.15$ mH, $L_M = 5.2$ mH.

5) Propeller parameters: D= 0.5 m, KT = –0.1060, KQ = –0.0186, $\rho = 1024$ kg/m3.

6) Diesel engine parameters: $K_y = 1.5e6$, 300 kW.

7) PI controller parameters of the governor: $K_p = 0.0077$, $K_I = 0.0165$.

8) Voltage regulator—exciter parameters: $K_p = 0.4$, $K_I = 0.2$, $T_{fb} = 0.01$ s, $T_{ff} = 1$ ms.

9) Photo voltaic array module parameters: $N_s=1000$, $N_p=10$, T_x(temperature)$=25^0$C, S_x(solar irradiation)$=400$.

REFERENCES

[1] Bijan Zahedi, *Student Member, IEEE*, and Lars E. Norum, *Member, IEEE"* Modeling and Simulation of All-Electric Ships With Low-Voltage DC Hybrid Power Systems ".

[2] J. M. Apsley, A. Gonzalez-Villasenor, M. Barnes, A. C. Smith, S.Williamson, J. D. Schuddebeurs, P. J. Norman, C. D. Booth, G. M. Burt, and J. R. McDonald, "Propulsion drive models for full electric marine propulsion systems," IEEE Trans. Ind. Appl., vol. 45, no. 2, pp. 676–684, Mar. 2009.

[3] S. De Breucker, E. Peeters, and J. Driesen, "Possible applications of plug-in hybrid electric ships," in Proc. IEEE Electric Ship Technol. Symp., Apr. 20–22, 2009, pp. 560–567.

[4] R. E. Hebner, "Electric ship power system—Research at the University of Texas at Austin," in Proc. IEEE Electric Ship Technol. Symp., Jul. 25–27, 2005, pp. 34–38.

[5] R. Nilsen and I. Sorfonn, "Hybrid power generation systems," in Proc. 13th Eur. Conf. Power Electron. Appl., Sep. 2009.

[6] G. Seenumani, H. Peng, and Sun, "A reference governor-based hierarchical control for failure mode power management of hybrid power systems for all-electric ships," *J. Power Sources*, vol. 196, no. 3, pp. 1599–1607, 2011.

[7] K. Hochkirch and V. Bertram, "Options for fuel saving for ships," Mare Forum: Maritime Transportation of Energy, Houston, TX, Feb. 19, 2010.

[8] Ph. Thounthong, S. Ra¨el, and B. Davat, "Energy management of fuel cell/battery/super capacitor hybrid power source for vehicle applications," J. Power Sources, vol. 193, no. 1, pp. 376–385, Aug. 2009.

[9] J.-S. Lai and D. J. Nelson, "Energy management power converters in hybrid electric and fuel cell vehicles," Proc. IEEE, vol. 95, no. 4, pp. 766–777, Apr. 2007.

[10] Muhammad H. Rashid, Power Electronics, Ph.D., Fellow IEE, Fellow IEEE.

[11] Robert W. Erickson, Fundamentals of Power Electronics. Norwell,, MA: Kluwer, 1999.

[12] B. Zahedi, O. C. Nebb, and L. E. Norum, "An isolated bidirectional converter modeling for hybrid electric ship simulations," in *Proc. IEEE Transp. Electrification Conf. Expo.*, Jun. 2012.

[13] H. A. Peterson and P. C. Krause, "A direct- and quadrature-axis representation of a parallel ac and dc power system," *IEEE Trans. Power App. Syst.*, vol. PAS-85, no. 3, pp. 210–225, Mar. 1966.

[14] P. C. Krause, O. Wasynczuk, and S. D. Sudhoff, Analysis of Electric Machinery and Drive Systems. Piscataway, NJ: IEEE Press/Wiley, 2002.

[15] H. Altas, and A.M. Sharaf "A Photovoltaic Array Simulation Model for Matlab-Simulink GUI Environment".

[16] J. F. Hansen, A. K. Adnanes, and T. I. Fossen, "Mathematical modeling of diesel-electric propulsion systems for marine vessels," *Math. Comput. Model. Dyn. Syst.*, vol. 7, no. 3, pp. 323–355, 2001.

[17] R. Ferreiro, M. Casado, and F. J.Velasco, "Trends on modelling techniques applied on ships propulsion systems monitoring," *J.Mar. Res.*, vol. 2, no. 1, pp. 87–104, 2005.

13611